

## Evaluation of $T$ -stress for cracks in elastic sheets

R. K. L. Su†

Department of Civil Engineering, The University of Hong Kong, Pokfulam Road, Hong Kong, PRC

(Received September 9, 2004, Accepted March 31, 2005)

**Abstract.** The  $T$ -stress of cracks in elastic sheets is solved by using the fractal finite element method (FFEM). The FFEM, which had been developed to determine the stress intensity factors of cracks, is re-applied to evaluate the  $T$ -stress which is one of the important fracture parameters. The FFEM combines an exterior finite element model with a localized inner model near the crack tip. The mesh geometry of the latter is self-similar in radial layers around the tip. The higher order Williams series is used to condense the large numbers of nodal displacements at the inner model near the crack tip to a small set of unknown coefficients. Numerical examples revealed that the present approach is simple and accurate for calculating the  $T$ -stresses and the stress intensity factors. Some errors of the  $T$ -stress solutions shown in the previous literature are identified and the new solutions for the  $T$ -stress calculations are presented.

**Key words:** eigenfunction expansion; interpolation; fractal; finite element; stress intensity factor;  $T$ -stress.

---

### 1. Introduction

Recently, much attention has been given on the determination of the elastic  $T$ -stress for cracked geometries (Karihaloo and Xiao 2001, Tan and Wang 2003, Chen *et al.* 2001). This stress corresponds to the first, non-singular term of Williams eigenfunction expansion series (Williams 1957) of the linear elastic stress field at the crack tip. The experimental results of Williams and Ewing (1972) and Ueda *et al.* (1983) on mixed mode loads showed that the inclusion of this term, which acted parallel to the crack at its tip, of the stress distribution could improve the accuracy for predicting the crack initiation angle and the critical stress intensity factor. Furthermore, this term was found to have significant effects on fracture toughness (Smith *et al.* 2001), size and shape of the crack-tip plastic zone (Larsson and Garlsson 1973, Rice 1974) and stability of the crack path direction (Cotterell and Rice 1980, Karihaloo and Keer 1981, Melin 2002). The application of both the stress intensity factor and the  $T$ -stress to include the constraint effect in failure investigations is becoming increasingly popular (Sherry *et al.* 1995). It is important to provide  $T$ -stress solutions for the cracked geometries under consideration. Several analytical and numerical methods have been developed to evaluate the  $T$ -stress for the cracked configurations. Leever and Radon (1982) used a variational technique to determine the unknown coefficients in the eigenfunction expansion series. Cardew *et al.* (1984) and later Kfoury (1986) used the path-independent interaction integral based on Eshelby's theory (1975) to calculate the  $T$ -stress. Sham (1991) and Wang (2002) employed the

---

† Assistant Professor, E-mail: [klsu@hkucc.hku.hk](mailto:klsu@hkucc.hku.hk)

higher order weight function method to solve the  $T$ -stress. Recently, Karihaloo and Xiao (2001) used the hybrid crack element, Tan and Wang (2003) used the quarter-point boundary element and Chen *et al.* (2001) employed the  $p$ -version finite element method to determine the  $T$ -stress with various cracked configurations. The compendiums of some common  $T$ -stress solutions have been presented (Sherry *et al.* 1995, Fett 1998).

The fractal finite element method (FFEM) which had been used to determine the stress intensity factors (Leung and Su 1994, 1995), in fact, can be re-applied to determine the elastic  $T$ -stress for different configurations of cracks in elastic sheets. The accuracy and efficient of the FFEM to solve the  $T$ -stress are validated by using four different numerical examples; all simulated with very coarse finite element meshes. Some errors shown on the previous compendium of the  $T$ -stress solutions are identified and the new interpolation functions for the determination of  $T$ -stress are presented.

## 2. A brief formulation of FFEM

The FFEM was originated in 1994 by Leung and Su to handle crack related problems. This method was modified from the two-level finite element method (Leung and Wong 1989) of which the principle was that, while the local interpolating shape function could reduce infinite number of degrees of freedom (DOF) within a finite element to finite number of the nodal displacements, the global interpolation function (the higher order Williams eigenfunction series) could further reduce the number of nodal displacements to a small set of unknown coefficients. The FFEM extended this concept by generating a self-similar mesh at the crack tip region (see Fig. 1) with infinite number of DOF around the singular point. It was discovered that the global stiffness in each layer of the inner model could be reduced via some algebra to that of the layer next to the outer finite element region (Leung and Su 1995). An infinite DOF could then be condensed expeditiously without increasing the order of the final equations as well as the computational time. The stress intensity factor was obtained directly from the generalized coordinates without any post-processing technique. The mesh generated by infinite number of geometric objects of similar shape was known as a fractal mesh. The numerical method being used was the two-level finite element method. Therefore, the method was named as the fractal two-level finite element method. This novel method had not only been used to determine the stress intensity factors but also been extended to solve various engineering problems such as dynamic crack problem (Hu *et al.* 1998), cracked structure-acoustic coupling problem (Zhong *et al.* 2003) and unbounded problems (Leung *et al.* 2004). Recently, this method was used to determine the numerical eigenfunctions for axisymmetrical cracked body for which the analytic eigenfunction cannot be found completely (Tsang *et al.* 2004). In this paper, this method is applied to calculate the  $T$ -stresses.

For completeness of the paper, brief formulation of the FFEM will be presented. To simplify our discussion, typical 9-node isoparametric elements with two DOF at each node will be used to illustrate the formulation of the FFEM. Based on the traditional finite element method (Cook *et al.* 1989), the first level interpolation in a finite element (say the  $l^{\text{th}}$  element) is achieved by using the conventional shape function  $\hat{\mathbf{N}}$ ,

$$\hat{\mathbf{u}}_{2 \times 1} = \hat{\mathbf{N}}_{2 \times 18} \hat{\mathbf{d}}_{18 \times 1} \quad (1)$$

where  $\hat{\mathbf{u}} = \{\hat{u}_x \hat{u}_y\}^T$  is the displacement vector in the  $l^{\text{th}}$  element and  $\hat{\mathbf{d}} = \{\dots \hat{v}_x^k \hat{v}_y^k \dots\}^T$  is the

nodal displacement vector. The symbol ‘ $\wedge$ ’ used here is to denote the vector or matrix in element level. Furthermore, considering the nodal displacement  $\hat{\mathbf{v}}^k = \{\hat{v}_x^k \hat{v}_y^k\}^T$  at the  $k^{\text{th}}$  node of the element; the displacement can be represented by the global interpolation, hence,

$$\hat{\mathbf{v}}_{2 \times 1}^k = \hat{\mathbf{T}}_{2 \times 2(N+1)}^k \bar{\mathbf{a}}_{2(N+1) \times 1} \quad (2)$$

where  $\bar{\mathbf{a}} = \{a_0 \ b_0 \ a_1 \ b_1 \ a_2 \ \dots\}^T$  is the unknown coefficient vector of the Williams eigenfunction series. The first two coefficients  $a_0$  and  $b_0$  are associated with the rigid body motions at the crack tip of the fractal mesh. The symbol ‘ $-$ ’ denotes the vector or matrix for the fractal mesh in global level. The explicit form of the global interpolation function  $\hat{\mathbf{T}}^k$  can be expressed as,

$$\hat{\mathbf{T}}^k = \frac{1}{2\mu} \begin{bmatrix} 1 & 0 & \dots & r^{\frac{n}{2}} \left[ \left( \kappa + \frac{n}{2} + (-1)^n \right) \cos \frac{n\theta}{2} - \frac{n}{2} \cos \left( \frac{n-4}{2} \theta \right) \right] \\ 0 & 1 & \dots & r^{\frac{n}{2}} \left[ \left( \kappa - \frac{n}{2} - (-1)^n \right) \sin \frac{n\theta}{2} + \frac{n}{2} \sin \left( \frac{n-4}{2} \theta \right) \right] \\ -r^{\frac{n}{2}} \left[ \left( \kappa + \frac{n}{2} - (-1)^n \right) \sin \frac{n\theta}{2} - \frac{n}{2} \sin \left( \frac{n-4}{2} \theta \right) \right] & \dots & & \\ r^{\frac{n}{2}} \left[ \left( \kappa - \frac{n}{2} + (-1)^n \right) \cos \frac{n\theta}{2} + \frac{n}{2} \cos \left( \frac{n-4}{2} \theta \right) \right] & \dots & & \end{bmatrix} \quad n = 1 \dots N \quad (3)$$

where  $r$  and  $\theta$  are the polar coordinates evaluated at the  $k^{\text{th}}$  node of the element,  $\mu$  is the shear modulus,  $\nu$  is Poisson’s ratio and  $\kappa = (3 - 4\nu)$  for plane strain condition and  $(3 - \nu)/(1 + \nu)$  for plane stress condition. It is noted that as a usually large amount of conventional finite elements is required to simulate the singular behaviour at the crack tip, the order of nodal displacement vector in the singular region is in general much larger than that of  $\bar{\mathbf{a}}$ . When an infinite number of the self-similar layers of elements is generated around the crack tip (as shown in Fig. 1) and is leading to infinite number of unknown displacements, Eq. (2) would be very helpful to condense the associated infinite number of DOF to a finite number of unknown coefficients  $\bar{\mathbf{a}}$ .

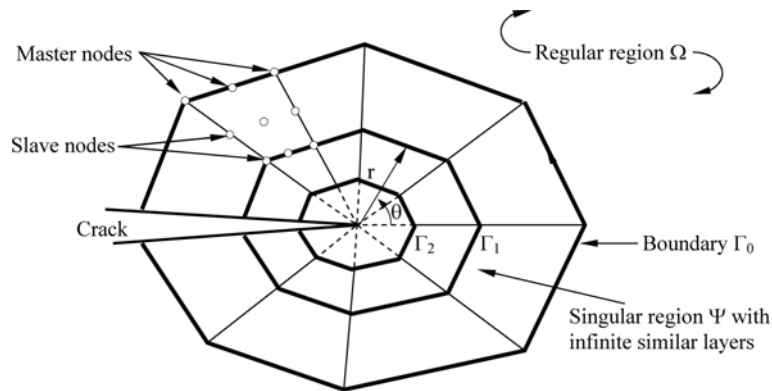


Fig. 1 Regular and singular regions and construction of fractal mesh

To perform the condensation, the elements on the first layer and the inner layers of the fractal mesh have to be considered separately. For the first layer of the fractal mesh, let there is  $M$  number of master nodes on the boundary  $\Gamma_0$ , the displacement vector associate with the master nodes is denoted as  $\{\hat{\mathbf{d}}_m\}_{2M \times 1}$  and the displacements within the boundary  $\Gamma_0$  (known as slave nodal displacements) is represented by  $\{\hat{\mathbf{d}}_s\}_{(18-2M) \times 1}$  as shown in Fig. 1. To carry out the condensation, the element stiffness matrix  $\hat{\mathbf{K}}^f$  of the first layer of mesh is first partitioned with respect to  $s$  and  $m$ ,

$$\hat{\mathbf{K}}_{18 \times 18}^f \hat{\mathbf{d}}_{18 \times 1} = \begin{bmatrix} \hat{\mathbf{K}}_{ss}^f & \hat{\mathbf{K}}_{sm}^f \\ \hat{\mathbf{K}}_{ms}^f & \hat{\mathbf{K}}_{mm}^f \end{bmatrix} \begin{Bmatrix} \hat{\mathbf{d}}_s \\ \hat{\mathbf{d}}_m \end{Bmatrix} \quad (4)$$

where the superscript  $f$  indicates the first layer of mesh. All the slave displacements would be condensed. The second level (global) interpolation of displacements can be written as follows,

$$\begin{Bmatrix} \hat{\mathbf{d}}_s \\ \hat{\mathbf{d}}_m \end{Bmatrix}_{18 \times 1} = \begin{bmatrix} \hat{\mathbf{T}}_{(18-2M) \times 2(N+1)}^f & \\ & \mathbf{I}_{2M \times 2M} \end{bmatrix} \begin{Bmatrix} \bar{\mathbf{a}} \\ \hat{\mathbf{d}}_m \end{Bmatrix}_{[2+2N+2M] \times 1} \quad (5)$$

Where  $\mathbf{I}$  is the identity matrix and  $\hat{\mathbf{T}}^f = \{\dots \hat{\mathbf{T}}^k \dots\}^T$  is the transformation matrix which can be obtained from Eq. (3). After condensing the stiffness matrix of the  $l^{\text{th}}$  element on the first layer of the fractal mesh, one has,

$$\hat{\mathbf{K}}_{(2+2N+2M) \times (2+2N+2M)}^f = \begin{bmatrix} \hat{\mathbf{T}}^{fT} \hat{\mathbf{K}}_{ss}^f \hat{\mathbf{T}}^f & \hat{\mathbf{T}}^{fT} \hat{\mathbf{K}}_{sm}^f \\ \text{sym} & \hat{\mathbf{K}}_{mm}^f \end{bmatrix} \quad (6)$$

Consider the inner elements located in the same sector of the  $l^{\text{th}}$  element (see Fig. 2), as there is no master node for the elements in the inner layers of the fractal mesh, all the DOF is transformed to the unknown coefficients. Due to the geometric self-similarity between successive layers of the fractal mesh, a simple geometric progression relationship was found for condensing and assembling all the inner layer elements (Leung and Su 1994), such that,

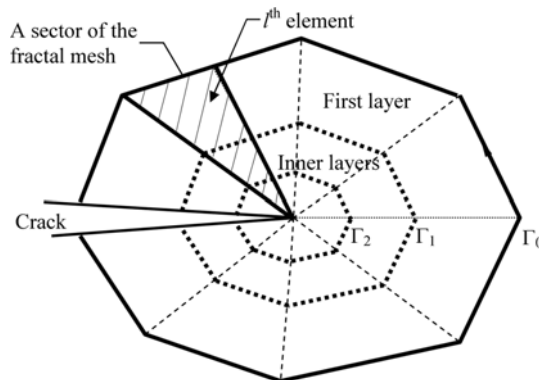


Fig. 2 A sector in the fractal mesh

$$\hat{\mathbf{K}}_{(2+2N) \times (2+2N)}^i = \begin{bmatrix} \vdots \\ \dots & \alpha_{ij} \hat{k}_{ij}^f & \dots \\ \vdots \end{bmatrix} \quad (7)$$

$$\alpha_{ij} = \begin{cases} 1 & \text{when } i_1 = 0 \text{ or } j_1 = 0 \\ \frac{1}{(2^{(i_1+j_1)} - 1)} & \text{else } i_1 = \text{Int}\left(\frac{i-1}{2}\right) \text{ and } j_1 = \text{Int}\left(\frac{j-1}{2}\right) \end{cases} \quad (8)$$

$$\hat{k}_{ij}^f \text{ is the } ij^{\text{th}} \text{ entry in } [\hat{\mathbf{T}}^f]_{2(N+1) \times 18}^T [\hat{\mathbf{K}}^f]_{18 \times 18} [\hat{\mathbf{T}}^f]_{18 \times 2(N+1)} \quad (9)$$

The generalized stiffness matrix  $\hat{\mathbf{K}}_s$  of that sector can be expressed as,

$$\hat{\mathbf{K}}_s \begin{Bmatrix} \bar{\mathbf{a}} \\ \hat{\mathbf{d}}_m \end{Bmatrix} = \begin{bmatrix} \hat{\mathbf{K}}^f + \hat{\mathbf{K}}^i & \hat{\mathbf{T}}^{fT} \hat{\mathbf{K}}_{sm}^f \\ \text{sym} & \hat{\mathbf{K}}_{mm}^f \end{bmatrix} \begin{Bmatrix} \bar{\mathbf{a}} \\ \hat{\mathbf{d}}_m \end{Bmatrix} \quad (10)$$

So far, only a sector of the elements along the perimeter  $\Gamma$ , as shown in Fig. 2, is condensed, the global generalized stiffness matrix  $\bar{\mathbf{K}}_s$  of the fractal mesh can be calculated by summing up the generalized stiffness matrix  $\hat{\mathbf{K}}_s$  associated with all the sectors, hence,

$$\bar{\mathbf{K}}_s \begin{Bmatrix} \bar{\mathbf{a}} \\ \bar{\mathbf{d}}_m \end{Bmatrix} = \left[ \sum_{\text{all sectors on } \Gamma_0} \hat{\mathbf{K}}_s \right] \begin{Bmatrix} \bar{\mathbf{a}} \\ \bar{\mathbf{d}}_m \end{Bmatrix} \quad (11)$$

By means of the master nodes, the singular region can be fit onto the regular region (see Fig. 1) which is modelled by the conventional finite elements. The unknown coefficients in Eq. (11) can be solved after applying the appropriate boundary conditions.

The stresses in the Cartesian coordinates at the crack tip can be expressed as an eigenfunction expansion series (Williams 1957),

$$\sigma_x = \frac{a_1}{\sqrt{r}} \cos \frac{\theta}{2} \left[ 1 - \sin \frac{\theta}{2} \sin \frac{3\theta}{2} \right] - \frac{b_1}{\sqrt{r}} \sin \frac{\theta}{2} \left[ 2 + \cos \frac{\theta}{2} \cos \frac{3\theta}{2} \right] + 4a_2 + O(r^{1/2}) \quad (12)$$

$$\sigma_y = \frac{a_1}{\sqrt{r}} \cos \frac{\theta}{2} \left[ 1 + \sin \frac{\theta}{2} \sin \frac{3\theta}{2} \right] + \frac{b_1}{\sqrt{r}} \sin \frac{\theta}{2} \cos \frac{\theta}{2} \cos \frac{3\theta}{2} + O(r^{1/2}) \quad (13)$$

$$\tau_{xy} = \frac{a_1}{\sqrt{r}} \sin \frac{\theta}{2} \cos \frac{\theta}{2} \cos \frac{3\theta}{2} + \frac{b_1}{\sqrt{r}} \cos \frac{\theta}{2} \left[ 1 - \sin \frac{\theta}{2} \sin \frac{3\theta}{2} \right] + O(r^{1/2}) \quad (14)$$

where  $O(r^{1/2})$  are the higher order terms near the crack tip. Invoking the definitions of the stress intensity factors and the  $T$ -stress, those fracture parameters can be related to the generalized coefficients as,

$$K_I = a_1 \sqrt{2\pi}, \quad K_{II} = -b_1 \sqrt{2\pi} \quad \text{and} \quad T = 4a_2 \quad (15)$$

### 3. Numerical examples

In order to verify the accuracy and the efficiency of the present method for determination of the  $T$ -stress, four numerical examples as shown in Fig. 3 are studied by the FFEM. They are (a) the centre crack in tension (CCT), (b) the double edge cracks in tension (DECT), (c) the single edge crack in tension (SECT) and (d) the single edge crack in bending (SECB). For problems (a) and (b) the aspect ratios  $H/W$  are taken as 1 and 3 whereas for problems (c) and (d) the aspect ratio  $H/W$  is taken as 6.

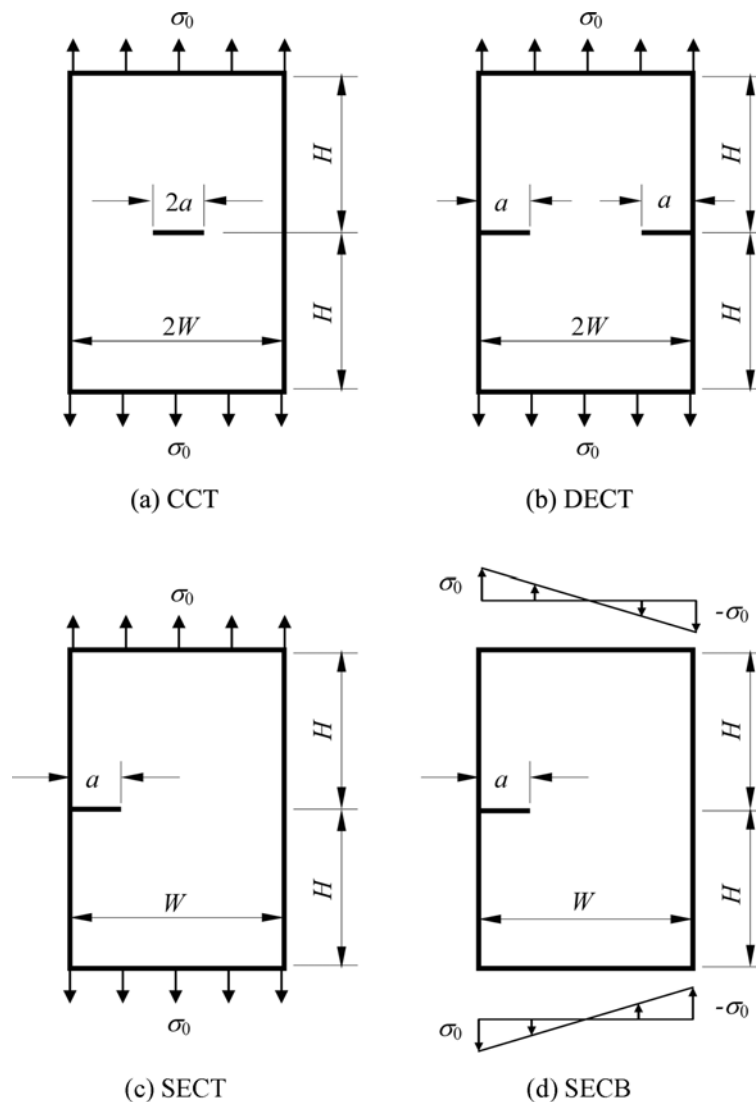


Fig. 3 Example problems for  $T$ -stress calculation: (a) Centre Crack Tension (CCT);  $H/W = 1$  and 3, (b) Double Edge Crack Tension (DECT);  $H/W = 1$  and 3, (c) Single Edge Crack Tension (SECT);  $H/W = 6$  and (d) Single Edge Crack Bending (SECB);  $H/W = 6$

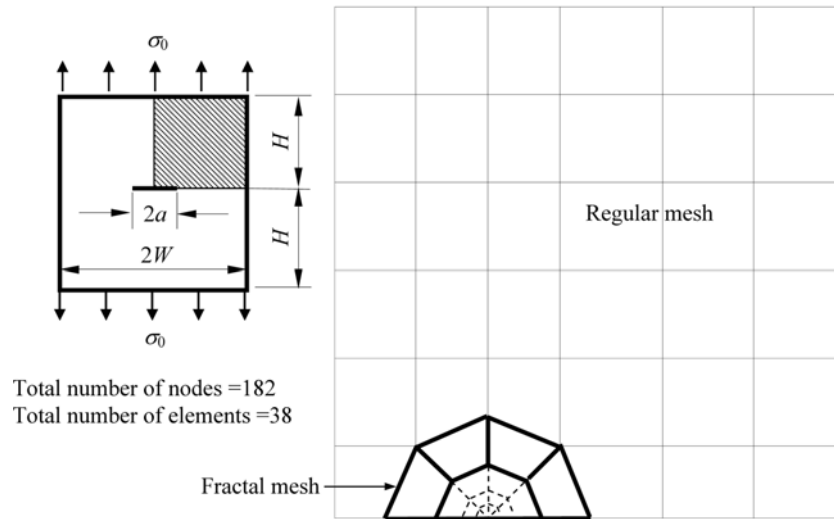


Fig. 4 The finite element mesh for a quarter of cracked sheet:  $H/W = 1$  and  $a/W = 0.3$

The FFEM calculation is performed for the problem of CCT. To verify the present approach, the crack configuration with crack length to sheet width ratio  $a/W = 0.05$  is selected to simulate an infinite sheet with a finite centred crack of which the analytical solution is  $T/\sigma_0 = -1$  (Leevers and Radon 1982). Due to symmetry, only a quarter of the sheet is modelled. The stress ratio  $T/\sigma_0$  calculated by FFEM is  $-1.0019$  which agrees well with the analytical solution.

The numerical results of CCT with crack length to sheet width ratio  $a/W$  varied from 0.1 to 0.7 had been presented (Tan and Wang 2003, Chen *et al.* 2001). Sherry *et al.* (1995) reported a compendium of the  $T$ -stresses and the stress biaxiality ratios  $B = T\sqrt{\pi a}/K_I$  for common crack configurations. Some of the previous results (Leevers and Radon 1982, Cardew *et al.* 1984, Kfourri 1986) presented  $B$  values only which were considered not particularly convenient for uses as the stress intensity factor had to be obtained from other handbooks. Sherry *et al.* (1995) had converted all the  $B$  values to the corresponding  $T/\sigma_0$  values and presented the  $T$ -stress results. The finite element mesh used in the FFEM calculation with  $a/W = 0.3$  and  $H/W = 1$  is shown in Fig. 4. The total numbers of conventional 9-node elements and fractal elements are 34 and 4 respectively. The

Table 1 Computed values of  $K_I$ ,  $T$  and  $B$  for CCT:  $H/W = 1$  and  $a/W = 0.3$

Sources	$\frac{K_I}{\sigma_0\sqrt{\pi a}}$	$\frac{T}{\sigma_0}$	$B = \frac{T\sqrt{\pi a}}{K_I}$
Present	1.1221	-1.154	-1.0284
Leevers and Radon (1982)	--	-1.088*	-1.0289
Cardew <i>et al.</i> (1984)	--	-1.093*	-1.032
Kfourri (1986)	--	-1.076*	-1.018
Fett (1998)	--	-1.1557	-1.028
Chen <i>et al.</i> (2001)	1.1231	-1.15536	-1.0286

\*values converted from the corresponding stress biaxiality ratio  $B$  by Sherry *et al.* (1995)

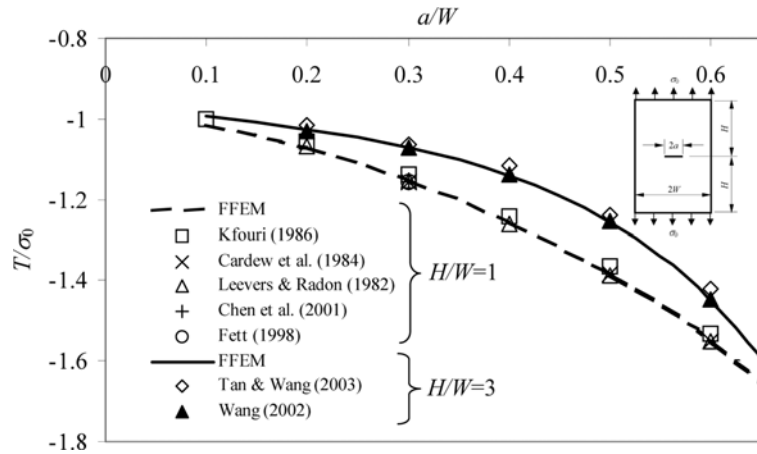


Fig. 5 The effect of  $a/W$  on  $T/\sigma_0$  for the problem of CCT

total number of nodes is 182 and the highest term used in the Williams series is  $N = 12$ . It is noted that extensive convergence and parametric studies (Leung and Su 1996, Xie *et al.* 2003) have been conducted and the mesh configuration of 4 elements per single layer of fractal mesh has been shown to be sufficient to achieve accurate results (with errors less than 3% for both  $K_I$  and  $K_{II}$ ) in the FFEM calculation. A comparison of the numerical values of the dimensionless stress intensity factors  $K_I/\sigma_0\sqrt{\pi a}$ , the dimensionless  $T$ -stress  $T/\sigma_0$  and the stress biaxiality ratio  $B = T\sqrt{\pi a}/K_I$  of CCT of aspect ratio  $H/W = 1$  and crack length ratio  $a/w = 0.3$  is shown in Table 1. Very good agreements with generally less than 1% differences are found between the present results and those available in the literature. However, inconsistent results are discovered for  $T/\sigma_0$  ratios obtained from Sherry *et al.* (1995). The discrepancy may be due to the inaccuracy of the stress intensity factors chosen for calculating  $T$ -stresses.

Fig. 5 shows the variations of  $T$ -stress against the crack length to sheet width ratio  $a/W$ . Consistent results are found for different aspect ratios ( $H/W$ ) and crack length ratios ( $a/W$ ). Based on our results, new functions of  $T/\sigma_0$  in terms of  $a/w$  are derived for CCT,

$$H/W = 1$$

$$\frac{T}{\sigma_0} = -0.8658 - 2.6851\frac{a}{w} + 17.011\left(\frac{a}{w}\right)^2 - 60.117\left(\frac{a}{w}\right)^3 + 91.223\left(\frac{a}{w}\right)^4 - 51.779\left(\frac{a}{w}\right)^5 \quad (16)$$

$$H/W = 3$$

$$\frac{T}{\sigma_0} = -0.8263 - 3.0809\frac{a}{w} + 19.391\left(\frac{a}{w}\right)^2 - 60.504\left(\frac{a}{w}\right)^3 + 84.718\left(\frac{a}{w}\right)^4 - 47.093\left(\frac{a}{w}\right)^5 \quad (17)$$

The FFEM calculation was conducted for the problem of DECT with crack length to sheet width ratio  $a/W$  varied from 0.1 to 0.7. The numerical results of the present methods and the other results available in the literature for  $H/W = 1$  and 3, and  $a/w = 0.5$  are shown in Table 2. Reasonable good agreements with differences less than around 3% are found. Again, similar discrepancy is found for

Table 2 Computed values of  $K_I$ ,  $T$  and  $B$  for DECT:  $a/W = 0.5$

Sources	$\frac{K_I}{\sigma_0 \sqrt{\pi a}}$	$\frac{T}{\sigma_0}$	$B = \frac{T \sqrt{\pi a}}{K_I}$
$H/W = 1$			
Present	1.332	-0.3172	-0.238
Leevers and Carlsson (1973)	--	--	-0.255
Kfouri (1986)	--	-0.2716*	-0.233
$H/W = 3$			
Present	1.169	-0.5523	-0.4727
Tan and Wang (2003)	--	-0.534	--
Wang (2002)	--	-0.553	--

\*value converted from the corresponding stress biaxiality ratio  $B$  by Sherry *et al.* (1995)

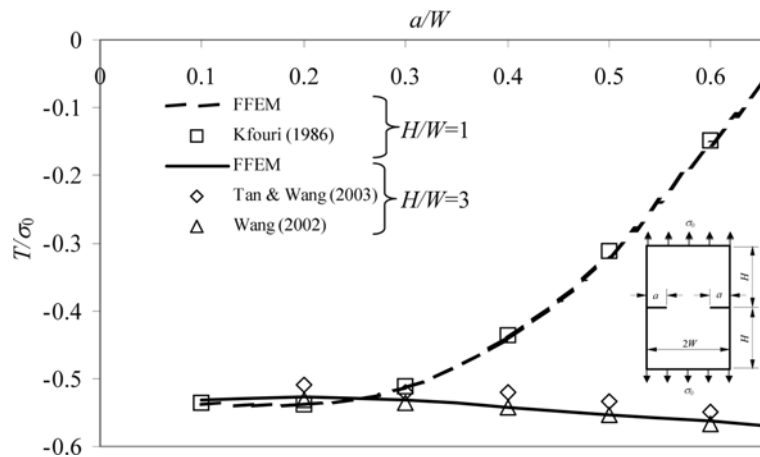


Fig. 6 The effect of  $a/W$  on  $T/\sigma_0$  for the problem of DECT

the interpolation results of Sherry *et al.* (1995). Fig. 6 shows the variations of  $T$ -stress against the crack length ratio  $a/W$  for DECT. Consistent results with those from Kfouri (1986) and Wang (2002) are observed in full ranges of aspect ratios ( $H/W$ ) and crack length to sheet width ratios ( $a/W$ ). However, higher discrepancies of around 3% are revealed for the present results and those from Tan and Wang (2003) which were obtained from the quarter-point boundary elements. Based on our results, new functions of  $T/\sigma_0$  in terms of  $a/w$  are proposed for DECT,

$$H/W=1$$

$$\frac{T}{\sigma_0} = -0.5622 + 0.5686 \frac{a}{w} - 4.4388 \left(\frac{a}{w}\right)^2 + 12.977 \left(\frac{a}{w}\right)^3 - 9.0093 \left(\frac{a}{w}\right)^4 + 0.3846 \left(\frac{a}{w}\right)^5 \quad (18)$$

$$H/W=3$$

$$\frac{T}{\sigma_0} = -0.5369 + 0.0373 \frac{a}{w} + 0.637 \left(\frac{a}{w}\right)^2 - 4.1959 \left(\frac{a}{w}\right)^3 + 7.499 \left(\frac{a}{w}\right)^4 - 4.4006 \left(\frac{a}{w}\right)^5 \quad (19)$$

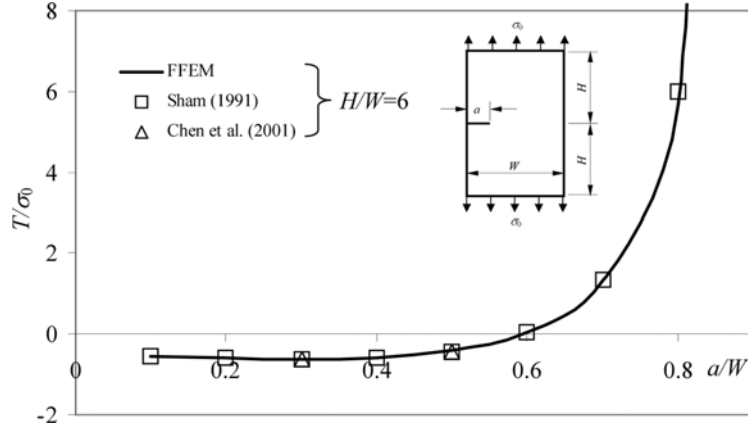


Fig. 7 The effect of  $a/W$  on  $T/\sigma_0$  for the problem of SECT

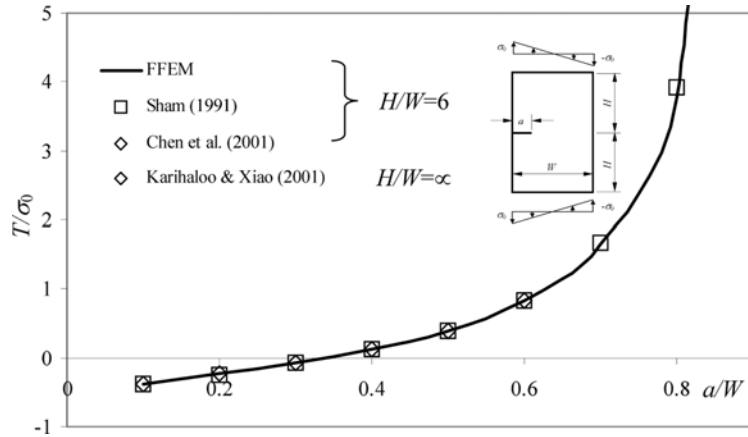


Fig. 8 The effect of  $a/W$  on  $T/\sigma_0$  for the problem of SECB

Single edge crack subjected to tension or bending moment is considered here. The problems had been studied by Sham (1991), Chen *et al.* (2001) and Karihaloo and Xiao (2001). For the case of cracked sheets subjected to bending, the maximum bending stress  $\sigma_0$  can be calculated by the formula  $\sigma_0 = 6M/(tW^2)$  where  $M$  is the applied end moment and  $t$  is the thickness of the sheet. Figs. 7 and 8 show the effects of  $a/W$  on the  $T$ -stresses for SECT and SECB respectively. Very good agreements with differences of around 2% are observed for all the results. It is noted that the infinitely long sheet considered by Karihaloo and Xiao (2001) gave very similar results to the case of  $H/W=6$ . It can be concluded that for SECB, the effect of aspect ratios on the  $T$ -stress is negligible when the ratio is higher than 6. It is noted that the interpolation functions of  $T/\sigma_0$  for single edge crack tension and bending moment are not available in the literatures, by using standard regression procedure, the interpolation functions are derived and expressed as follows,

SECT

$$\frac{T}{\sigma_0} = -0.69261 - 1.29643 \frac{a}{w} - 0.1199 \left(\frac{a}{w}\right)^2 - \frac{0.22305 - 0.20418a/w}{(a/w - 1)^3} \tag{20}$$

## SECB

$$\frac{T}{\sigma_0} = -0.59793 + 0.70080\frac{a}{w} + 0.68887\left(\frac{a}{w}\right)^2 - \frac{0.11637 - 0.11175a/w}{(a/w - 1)^3} \quad (21)$$

The interpolation errors of the above two equations are generally less than 3% in the range of  $0.1 \leq a/w \leq 0.8$ .

#### 4. Conclusions

By using the FFEM, the  $T$ -stresses for various crack configurations were evaluated. The explicit formulation of FFEM has been described. Using relatively coarse meshes, the  $T$ -stresses were determined for the problems of CCT, DECT, SECT and SECB. The present method has shown good agreements with the higher order weight functions method, the Eshelby's path-independent interaction integral method, the hybrid crack element and the  $p$ -version finite element method. The numerical examples further revealed that the present method is simple, accurate and reliable for solving  $T$ -stresses under different loading conditions. The present study discovered some of the errors presented in the previous literature and the new interpolation functions for the determination of  $T$ -stresses were derived.

#### Acknowledgements

The work described in this paper was fully supported by the grant from the University Research Grants (URG) through the small project funding 2004-05, The University of Hong Kong.

#### References

- Cardew, G.E., Goldthorpe, M.R., Howard, I.C. and Kfoury, A.P. (1984), *On the Elastic T-term. Fundamentals of Deformation and Fracture*, In: Bilby, B.A., Miller, K.J. and Willis, J.R. editors, Cambridge University Press, Cambridge.
- Chen, C.S., Krause, R., Pettit, R.G., Banks-Sills, L. and Ingrassia, A.R. (2001), "Numerical assessment of  $T$ -stress computation using a  $p$ -version finite element method", *Int. J. Fracture*, **107**(2), 177-199.
- Cook, R.D., Malkus, D.S. and Plesha, M.E. (1989), *Concepts and Applications of Finite Element Analysis*, 3rd Edition, John Wiley & Son, New York.
- Cotterell, B. and Rice, J.R. (1980), "Slightly curved or kinked cracks", *Int. J. Fracture*, **16**(2), 155-169.
- Eshelby, J.D. (1975), *The Calculation of Energy Release Rates*. In: Sih G.C., van Elst, H.C., Broek, D., editors. *Prospects of Fracture Mechanics*. Noordhoff International.
- Fett, T. (1998), "A compendium of  $T$ -stress solutions", Technical Report FZKA 6057, Institut für Materialforschung.
- Hu, C.B., Li, Y.T. and Gong, J. (1998), "The transition method of geometrically similar element for dynamic crack problem", *Fracture and Strength of Solids, Pts 1 and 2 Key Engineering Materials*, **145-9**, 267-272.
- Karihaloo, B.L., Keer, L.M., Nemat-Nasser, S. and Oranratnachai, A. (1981), "Approximate description of crack kinking and curving", *J. Appl. Mech. -Transactions of the ASME*, **48**(3), 515-519.
- Karihaloo, B.L. and Xiao, Q.Z. (2001), "Higher order terms of the crack tip asymptotic field for a notched three-point-bend beam", *Int. J. Fracture*, **112**(2), 111-128.

- Kfoury, A.P. (1986), "Some evaluations of the elastic  $T$ -term using Eshelby's method", *Int. J. Fracture*, **30**(4), 301-315.
- Larsson, S.G. and Carlsson, A.J. (1973), "Influence of non-singular stress terms and specimen geometry on small-scale yielding at crack-tips in elastic-plastic materials", *J. of the Mechanics and Physics of Solids*, **21**(4) 263-277.
- Leevers, P.S. and Radon, J.C. (1982), "Inherent stress biaxiality in various fracture specimen geometries", *Int. J. Fracture*, **19**(4), 311-325.
- Leung, A.Y.T., Dai, H., Fok, S.L. and Su, R.K.L. (2004), "The fractal finite element method for unbounded problems", *Int. J. for Numer. Meth. Eng.*, **61**(7), 990-1008.
- Leung, A.Y.T. and Su, R.K.L. (1994), "Mode I crack problems by fractal two-level finite element methods", *Engineering Fracture Mechanics*, **48**(6), 847-856.
- Leung, A.Y.T. and Su, R.K.L. (1995), "Mixed mode two-dimensional crack problems by fractal two-level finite element method", *Engineering Fracture Mechanics*, **51**(6), 889-895.
- Leung, A.Y.T. and Su, R.K.L. (1996), "Fractal two-level finite element method for two-dimensional cracks", *Microcomputers in Civil Engineering*, **11**(4), 249-257.
- Leung, A.Y.T. and Wong, S.C. (1989), "Two-level finite element method for plane cracks", *Communications in Applied Numerical Methods*, **5**(4), 263-274.
- Melin, S. (2002), "The influence of the  $T$ -stress on the directional stability of cracks", *Int. J. Fracture*, **114**(3), 259-265.
- Rice, J.R. (1974), "Limitations to the small scale yielding approximation for crack tip plasticity", *J. of the Mechanics and Physics of Solids*, **22**(1), 17-26.
- Sham, T.L. (1991), "The determination of the elastic  $T$ -term using higher order weight functions", *Int. J. Fracture*, **48**(2), 81-102.
- Sherry, A.H., France, C.C. and Goldthorpe, M.R. (1995) "Compendium of  $T$ -stress solutions for two and three-dimensional cracked geometries", *Fatigue & Fracture of Engineering Materials & Structures*, **18**(1), 141-155.
- Smith, D.J., Ayatollahi, M.R. and Pavier, M.J. (2001), "The role of  $T$ -stress in brittle fracture for linear elastic materials under mixed-mode loading", *Fatigue & Fracture of Engineering Materials & Structures*, **24**(2), 137-150.
- Tan, C.L. and Wang, X. (2003), "The use of quarter-point crack tip elements for  $T$ -stress determination in boundary element method analysis", *Engineering Fracture Mechanics*, **70**(15), 2247-2252.
- Tsang, D.K.L., Oyadiji, S.O. and Leung, A.Y.T. (2004), "Applications of numerical eigenfunctions in the fractal-like finite element method", *Int. J. Numer. Meth. Eng.*, **61**(4), 475-495.
- Ueda, Y., Ikeda, K. and Yao, T. (1983), "Characteristics of brittle fracture under general combined modes including those under bi-axial tensile loads", *Engineering Fracture Mechanics*, **18**(6), 1131-1158.
- Wang, X. (2002), "Elastic  $T$ -stress for cracks in test specimens subjected to non-uniform stress distribution", *Engineering Fracture Mechanics*, **69**(12), 1339-1352.
- Williams, J.G. and Ewing, P.D. (1972), "Fracture under complex stress – the angled crack problem", *Int. J. Fracture Mechanics*, **8**(4), 441-446.
- Williams, M.L. (1957), "On the stress distribution at the base of a stationary crack", *J. Appl. Mech.*, ASME, **24**, 109-114.
- Xie, J.F., Fok, S.L. and Leung, A.Y.T. (2003), "A parametric study on the fractal finite element method for two-dimensional crack problems", *Int. J. Numer. Meth. Eng.*, **58**(4), 631-642.
- Zhong, W.F., Wu, Y.D., Wu, G.R. and Liang, Y.D. (2003), "Analysis on acoustical scattering by a cracked elastic structure", *ACTA Mechanica Solida Sinica*, **16**(3), 262-268.